

The effect of rotation on the abundances of the chemical elements of the A–type stars in the Praesepe cluster[★]

L. Fossati¹, S. Bagnulo², J. Landstreet⁴, G. Wade⁵, O. Kochukhov⁶, R. Monier⁷, W. Weiss¹, and M. Gebran⁸

¹ Institut für Astronomie, Universität Wien, Türkenschanzstrasse 17, 1180 Wien, Austria.
e-mail: fossati@astro.univie.ac.at; weiss@astro.univie.ac.at

² Armagh Observatory, College Hill, Armagh BT61 9DG, Northern Ireland. e-mail: sba@arm.ac.uk

³ Department of Physics & Astronomy, University of Western Ontario, London, N6A 3K7, Ontario, Canada.
e-mail: jlandstr@astro.uwo.ca

⁴ Physics Dept., Royal Military College of Canada, PO Box 17000, Station Forces, K7K 4B4, Kingston, Canada. e-mail: Gregg.Wade@rmc.ca

⁵ Department of Physics and Astronomy, Uppsala University, 751 20, Uppsala, Sweden. e-mail: oleg@astro.uu.se

⁶ Laboratoire Universitaire d’Astrophysique de Nice, Université de Nice Sophia–Antipolis, Parc Valrose, 06000 Nice, France. e-mail: Richard.MONIER@unice.fr

⁷ Groupe de Recherche en Astronomie et Astrophysique du Languedoc, UMR 5024, Université Montpellier II, Place Eugène Bataillon, 34095 Montpellier, France. e-mail: Marwan.Gebran@graal.univ-montp2.fr

ABSTRACT

Aims. We study how chemical abundances of late B–, A– and early F–type stars evolve with time, and we search for correlations between the abundance of chemical elements and other stellar parameters, such as effective temperature and $v \sin i$.

Methods. We have observed a large number of B–, A– and F–type stars belonging to open clusters of different ages. In this paper we concentrate on the Praesepe cluster ($\log t = 8.85$), for which we have obtained high resolution, high signal-to-noise ratio spectra of sixteen normal A– and F–type stars and one Am star, using the SOPHIE spectrograph of the Observatoire de Haute–Provence. For all the observed stars, we have derived fundamental parameters and chemical abundances. In addition, we discuss another eight Am stars belonging to the same cluster, for which the abundance analysis had been presented in a previous paper.

Results. We find a strong correlation between peculiarity of Am stars and $v \sin i$. The abundance of the elements underabundant in Am stars increases with $v \sin i$, while it decreases for the overabundant elements. Chemical abundances of various elements appear correlated with the iron abundance.

1. Introduction

In stellar astrophysics, the study of the atmospheres of A– and B–type stars plays a very special role. The atmospheres of these stars display a variety of different phenomena, such as the presence of large and relatively simple magnetic fields, strong surface convection, pulsation, diffusion of chemical elements, and various kinds of mixing processes from small-scale turbulence to global circulation currents. These general physical processes are almost certainly active in the atmospheres (and interiors) of stars other than the main sequence A– and B–type stars, but in more subtle ways. Because of the easily visible effects found in A– and B–type stars, these stars provide unique access to the invisible interior processes. To fully understand the actual role of all these physical phenomena, it is very important to seek constraints from the observations, in particular to perform a detailed study of a large number of stars of different ages and peculiarity types.

For this project, it is very interesting to study stars that are cluster members, rather than selecting targets in the field, because of two very compelling reasons. First, we can assume that all cluster members have approximately the same original chemical composition and age. Therefore, when we analyse the chemical abundances of stars belonging to the same cluster, we can assume that we are studying objects that are different only

by their initial mass, rotational velocity, magnetic field strength and binarity. Second, the age of stars belonging to open clusters can be determined with much higher accuracy than for objects in the field, especially for stars that are young enough that less than half of their life in the main sequence has elapsed (for a discussion of the star’s age determination see Bagnulo et al. 2006). Therefore, we have carried out two large observational campaigns. With FORS1 at the ESO VLT and with ESPaDOnS at the Canada–France–Hawaii Telescope (CFHT) we have made a survey of magnetic A– and B–type stars in open clusters, to search for links between magnetic fields and stellar evolution. The results of this campaign are described by Bagnulo et al. (2006); Landstreet et al. (2007, 2008). In the framework of this observational campaign, we have also obtained high-resolution spectroscopy of a large number of early-type stars in about ten open clusters of different ages. The clusters are approximately uniformly distributed in logarithmic age from $\log t = 6.8$ to $\log t = 8.9$, and the spectra have been obtained using five different spectrographs: FLAMES at the ESO VLT, FIES at the Nordic Optical Telescope (NOT), ELODIE and SOPHIE at the Observatoire de Haute–Provence (OHP), and ESPaDOnS at the CFHT.

In a previous paper (Fossati et al. 2007, hereafter referred to as Paper I), we started the analysis of the Praesepe cluster, presenting the observations and the results of the abundance analysis of eight Am and three normal A– and F–type stars. In this

work we complete the study of the Praesepe cluster by presenting observations of 16 additional normal A- and early F-type stars, and an additional Am star. These new observations were obtained with the SOPHIE spectrograph at the Observatoire de Haute-Provence. Because of the large sample of analysed stars, we are able to make a sensitive search for correlations between the abundances of the chemical elements and other stellar parameters, such as the effective temperature T_{eff} and projected rotational velocity $v \sin i$.

This Paper is organised as follows. In Sect. 2 we describe the criteria that we have adopted for target selection, which were used both for the entire observational campaign, and for the specific observations of the Praesepe cluster presented in this paper. Details about observations of the Praesepe cluster and data reduction are given in Sect. 3. In Sect. 4 we compare spectra of a reference star obtained with two different instruments that we have used in our observational campaign: the SOPHIE spectrograph and the ESPaDOnS spectropolarimeter. In Sect. 5 we describe the procedure used to perform the abundance analysis, and we present the results obtained for the early-type stars of the Praesepe cluster observed with the SOPHIE spectrograph. In Sect. 6 we consider the abundances of chemical elements for the stars studied in Paper I and for the stars studied in this work. We search for correlations between chemical element abundances and effective temperature, $v \sin i$, M/M_{\odot} and fractional age (τ – fraction of main sequence lifetime completed). In Sect. 7 we summarise our conclusions.

2. Target selection

For target selection in the overall program, we assigned the highest priority to the most probable cluster members that were already known to be chemically peculiar (Am, Ap, HgMn stars) and/or to show slow rotation (typically $v \sin i < 50 \text{ km s}^{-1}$). For this purpose we have followed a standard procedure to select the stars to observe and to assign their priority.

The first step was to identify the most probable cluster members by checking the membership probabilities given by Robichon et al. (1999) and Baumgardt et al. (2000) obtained from HIPPARCOS data, by Kharchenko et al. (2004) and by Dias et al. (2006). We considered as probable members of the cluster every star with a kinematic and photometric membership probability higher than 0.14 (Kharchenko, private communication) in the case of the Kharchenko et al. (2004) catalogue, or a membership probability higher than 10% for the Dias et al. (2006) catalogue.

We then searched for information about the spectral type, magnitude, $v \sin i$, binarity, variability, chemical peculiarities, magnetic field and radial velocity for each star considered a probable member of the cluster. We collected information from SIMBAD¹ (scanning also the different references mentioned therein), VIZIER² (using a combination of several keywords – binaries:cataclysmic, binaries:eclipsing, binaries:spectroscopic, multiple_stars, open_clusters, positional_data, proper_motions, rotational_velocities, spectral_classification, spectrophotometry, spectroscopy, stars:early-type, stars:late-type, stars:peculiar, stars:variable – in a range of 10 arcsec around the position of each star) and the WEBDA³ database (Mermilliod & Paunzen 2003). We have also looked for additional information about each star in articles by Glebocki & Stawikowski (2000) and

Royer et al. (2002) for $v \sin i$ measurements, Rodríguez et al. (2000) for δ Sct pulsations, the SB9 catalogue (Pourbaix et al. 2004) for information about a possible binarity and Renson et al. (1991) for chemical peculiarities.

We have then searched for archival high resolution spectra in several archives (e.g. the ESO archive⁴ and the ELODIE archive⁵), in order to avoid a duplication of observational effort, in case some stars had already been observed with high resolution spectroscopy. Almost no pre-existing spectra were found.

Of the sample obtained with this procedure, we kept only the stars with spectral types between F5 (to avoid too long an exposure time on a single object) and B5 (to avoid strong stellar winds), giving a higher rank to peculiar stars and slow rotators. From the sample we have removed stars already known to be SB2 systems, unless they had already been extensively observed using high-resolution spectroscopy.

3. Observations and data reduction

We have observed seventeen stars of the Praesepe cluster using the SOPHIE spectrograph at the Observatoire de Haute-Provence (OHP) during two runs, from December 1st to 2nd 2006 and from March 10th to 12th 2007.

SOPHIE is a cross-dispersed échelle spectrograph mounted at the 1.93-m telescope at the OHP. The spectrograph is fed from the Cassegrain focus through a pair of optical fibers, one of which is used for starlight and the other can be used for either the sky background or the wavelength calibration lamp, but can also be masked. The spectra cover the wavelength range 3872–6943 Å. The instrument allows observations either with medium spectral resolution ($R \sim 40\,000$) or with high spectral resolution ($R \sim 75\,000$). Since for most of the stars of our sample no precise $v \sin i$ measurements were available, we decided to observe all of them in high resolution mode.

The spectra were automatically reduced using the SOPHIE pipeline, adapted from the HARPS software designed by Geneva Observatory. A detailed description of the pipeline is available on the SOPHIE web page⁶.

From our spectra we found that almost all of the stars have high rotational velocity ($v \sin i \geq 30 \text{ km s}^{-1}$). For these objects the continuum normalisation is a critical reduction procedure that cannot be performed with an automatic fitting procedure. We therefore rectified the continua of these stars manually. Even with manual rectification, it was not possible to determine a correct continuum level shortwards of the H γ line (4340.462 Å), since there were not enough continuum windows in the spectra, due to the crowding of spectral lines when $v \sin i$ is high.

It is well known how important it is to reach a high signal-to-noise ratio (SNR) to be able to carry out an abundance analysis of rapidly rotating stars (Hill & Landstreet 1993). For two stars (HD 73798 and HD 73993) the SNR was too low, so we have rebinned the spectra to increase the SNR, at the expense of spectral resolution.

The complete sample of stars observed and analysed in this paper is listed in Table 1. In the sample, one object is an Am star, while the others are normal stars with spectral types between F2 and A1. Seven stars of our sample are present in the δ Sct variable star catalog of Rodríguez et al. (2000). One star (HD 73993) is present in the Combined General Catalogue of Variable Stars (Samus & Durlevich 2004), but the variability type is listed as

¹ <http://simbad.u-strasbg.fr/simbad/sim-fid>

² <http://vizier.u-strasbg.fr/viz-bin/VizieR>

³ <http://www.univie.ac.at/webda/>

⁴ <http://archive.eso.org/>

⁵ <http://atlas.obs-hp.fr/elodie/>

⁶ <http://www.obs-hp.fr/www/guide/sophie/sophie-eng.html>

Table 1. Basic data of the observations for the program stars. The SNR are calculated at $\sim 5500 \text{ \AA}$ in a bin of 0.5 \AA . The exposure time is in seconds. The HJD indicate the Heliocentric Julian Date at the middle of the exposure. The δ Sct stars are present in the catalog of variable stars by Rodríguez et al. (2000). *: the star is included, as variable of an "unknown" type, in the Combined General Catalogue of Variable Stars by Samus & Durlevich (2004).

HD	HJD	M_v	Spectral Type	SNR	Exp. Time	Remarks
72757	2454172.336	8.45	F0	190	3600	
72846	2454070.737	7.48	A5V	210	3600	
73175	2454171.406	8.25	F0Vn	155	3600	δ Sct
73345	2454171.363	8.14	A7V	188	3600	δ Sct
73450	2454171.494	8.59	A9V	185	3600	δ Sct
73574	2454171.585	7.75	A8V	170	3600	
73666	2454070.682	6.61	A1V	326	1800	speckle binary
73746	2454172.514	8.72	F0V	154	3600	δ Sct
73798	2454172.424	8.48	F0V	190	3600	δ Sct
73993	2454171.450	8.56	F2V	134	3600	variable*
74028	2454171.318	7.97	A7V	185	3600	δ Sct
74050	2454170.566	7.91	A6Vn	160	3600	δ Sct
74135	2454172.559	8.88	F0	120	3600	
74587	2454172.468	8.51	A5	177	3600	
74589	2454172.379	8.46	F0	200	3600	
74656	2454170.537	8.04	Am	226	2x3600	sum of two exposures
74718	2454171.538	8.39	A5	172	3600	

"unknown". HD 73666 is the only known binary star present in our sample, as we have removed all SB2 stars from the selected target stars, as explained in Sect. 2.

4. SOPHIE vs. ESPaDOnS

The observational material employed in this large project has been obtained with different instruments at different telescopes. Since the homogeneity of the analysis is of crucial importance, in this section we compare spectra of a reference star obtained with two different spectrographs to demonstrate the homogeneity of our data.

HD 73666 was previously analysed in Paper I. The star was also used as reference star by Ryabchikova et al. (2008). Here we compare the spectra of HD 73666 obtained with ESPaDOnS (analysed in Paper I) and with SOPHIE. ESPaDOnS was mounted at the Canada-France-Hawaii Telescope (CFHT) in 2005 and SOPHIE at the Observatoire de Haute-Provence (OHP) in 2006. The two instruments have similar mean resolving power, 65 000 and 75 000 respectively. ESPaDOnS is also adapted for spectropolarimetric observations, while SOPHIE for radial velocity observations. Here we compare the spectra of the reference star obtained with the two instruments.

In Fig. 13 and Fig. 14 (available online) we show a direct comparison between the ESPaDOnS and SOPHIE spectra for HD 73666 around the He multiplet at $\sim 4471.5 \text{ \AA}$ and the strong Fe II line at 5018.440 \AA respectively. No significant differences are present apart from those due to the small difference of spectral resolution, visible mainly in the cores of the strong lines.

HD 73666 was first detected as a binary star with speckle interferometry by Hartkopf & McAlister (1984), and was observed and analysed further by McAlister et al. (1987). Mason et al. (1993), who collected all available interferometric measurements and concluded that HD 73666 "shows little orbital motion". Radial velocity measurements are reported by Abt (1970), Conti et al. (1974), Abt & Willmarth (1999) and Madsen et al. (2002). All these authors give radial velocities compatible with the cluster mean of $34.5 \pm 0.0 \text{ km s}^{-1}$ (Robichon et al. 1999). The spectra plotted in Fig. 13 and Fig. 14 have been corrected only for the terrestrial radial velocity; nevertheless, no radial velocity

difference is visible from the comparison of the two spectra, in agreement with results from previous authors.

5. Model atmosphere and abundance analysis

Model atmospheres were calculated with the LTE code LLMODELS, which uses direct sampling of the line opacities (Shulyak et al. 2004) and makes it possible to compute model atmospheres with an individualised abundance pattern. We adopted the VALD database (Piskunov et al. 1995; Kupka et al. 1999; Ryabchikova et al. 1999) as the source of spectral line data, including lines originating from predicted levels. We have carried out a preselection procedure to eliminate all lines that do not contribute significantly to the line opacity. This was done by requiring that the line-to-continuum opacity ratio at the center of each included line be greater than 0.05 %. Convection was treated according to the CM approach (Canuto & Mazzitelli 1992).

The initial values of the fundamental atmospheric parameters (T_{eff} and $\log g$) were derived from Strömgren (Hauck & Mermilliod 1998) and Geneva (Mermilliod & Paunzen 2003) photometry, using calibrations from Napiwotzki et al. (1993) and Kunzli et al. (1997) respectively.

The adopted T_{eff} and $\log g$ were derived spectroscopically, as explained in detail in Paper I. We have almost always used Fe lines for this purpose, as the generally high $v \sin i$ of the analysed stars did not provide a suitable number and variety of lines of other elements. The microturbulent velocity (v_{mic}) was determined spectroscopically, from Fe and Ti II lines, for HD 74656 only; this was possible because of its low $v \sin i$. For all other stars we have adopted v_{mic} computed from the relation (Pace et al. 2006):

$$v_{\text{mic}} = -4.7 \log(T_{\text{eff}}) + 20.9 \text{ km s}^{-1}. \quad (1)$$

There is no significant difference between adopting the v_{mic} given by Eq. 1 and assuming a fixed value of 2.7 km s^{-1} . We notice that v_{mic} obtained for the Am star HD 74656 is significantly larger than 2.7 km s^{-1} . Whether this is also the case for other stars of the sample cannot be tested with the available data.

Radial velocity (v_r) and $v \sin i$, in km s^{-1} , were determined by computing the median of the results obtained by synthetic fitting of several individual lines in the observed spectrum. We have derived error bars for these quantities for each analysed star using the standard deviation of the derived values. The error bar associated with v_r is strongly dependent on $v \sin i$, ranging from about 1 km s^{-1} for slow rotators, up to about 8 km s^{-1} for the fast rotators. The error bars in $v \sin i$ are about 5 % or 3 km s^{-1} , whichever is larger.

Table 2 reports the fundamental parameters obtained for each star of the sample from photometry and spectroscopy. The parameters adopted for abundance analysis are those obtained from spectroscopy.

We have tested the fundamental parameters adopted for the abundance analysis with spectrophotometry from Clampitt & Burstein (1997) for 5 stars of the sample. We used Atlas9 models and the fundamental parameters adopted for the abundance analysis to compute the fluxes for comparison with the spectrophotometry. The fluxes were normalised to the flux at 5560 \AA . An example of the comparison is shown in Fig. 1. We have found good agreement, within the error bars of the fundamental parameters, for all the stars for which spectrophotometry was available.

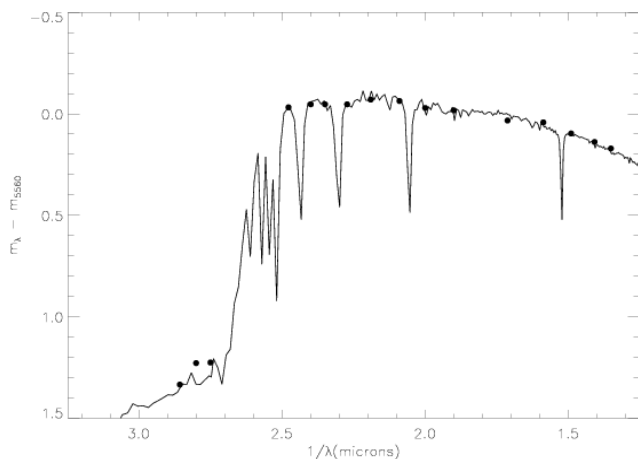


Fig. 1. Comparison between spectrophotometry from Clampitt & Burstein (1997) and normalised fluxes at 5560 \AA with the fundamental parameters adopted for the abundance analysis of the star HD 73345.

The synthetic line spectrum was produced with the synthesis code Synth3 (Kochukhov 2006). In each spectrum we have fit the cores of selected lines of each ion to obtain a value of the abundance associated with each line. The adopted abundance of that ion is then defined to be the mean of the abundances obtained from the selected lines. The error bars associated with the mean abundances are the standard deviations, and they do not include uncertainties in fundamental parameters (see below). The abundances and their standard error bars are given in Table 3.

The line data required for our analysis were extracted from the VALD database. Line parameters of the lines selected for the fundamental parameter derivation and abundance analysis were checked by synthesising these lines in the solar spectrum taken from the National Solar Observatory Atlas⁷. The lines for which

we found a discrepancy between the observed and synthesised solar spectrum were rejected.

The typical number of lines selected for the analysis varied according to the rotational velocity of the analysed star. The Fe abundance was always determined on the basis of the largest number of lines, in comparison with other elements. The number of lines used to derive the abundance of each element is given in Table 3, following the (internal) standard deviation associated with each measured abundance.

For all the elements that were not analysed we have adopted the solar abundance from Asplund et al. (2005). (This fact enters into the model atmosphere computation, and in the normalisation of the results expressed according to the total number of nuclei per unit volume N_{tot} .)

The high $v \sin i$ of some of the analysed stars resulted in a different and smaller selection of lines compared to the line list employed for slower rotators. We have checked if this is a source of systematic error by performing the abundance analysis of HD 73045 ($v \sin i = 10 \text{ km s}^{-1}$ – analysed in Paper I) and HD 73746 ($v \sin i = 95 \text{ km s}^{-1}$) adopting the line list used for HD 72757 ($v \sin i = 179 \text{ km s}^{-1}$). The results of this test, illustrated in Fig. 2, show that no systematic errors are introduced by the difference in selected lines.

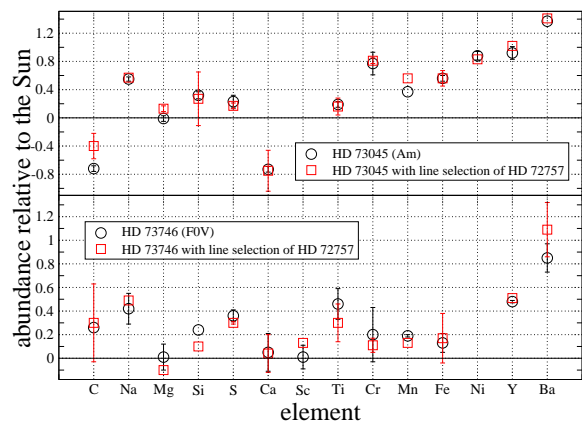


Fig. 2. Comparison between the abundances derived for HD 73045 ($v \sin i = 10 \text{ km s}^{-1}$ – open circles in the upper panel) and HD 73746 ($v \sin i = 95 \text{ km s}^{-1}$ – open circles in the lower panel) adopting a proper line selection and the lines used to determine the abundances of HD 72757 ($v \sin i = 179 \text{ km s}^{-1}$ – open squares in both panels).

The high rotational velocity of many of the analysed stars results in a line list dominated by strong and saturated lines. These lines are more sensitive to v_{mic} variations than shallow lines. For this reason the uncertainties of the adopted v_{mic} , T_{eff} , and $\log g$ values need to be considered to obtain a realistic estimate of the error bars associated with the derived element abundances.

In Paper I we have shown the results of two tests performed on slowly rotating stars. They show i) how the standard deviation from the mean Fe abundance changes for $v_{\text{mic}} = 0, 1, 2, \dots, 6 \text{ km s}^{-1}$, adopting fundamental parameters derived from photometry and spectroscopy and ii) the uncertainties introduced in the abundances of Fe, Ti and Ni by varying effective temperature

⁷ <http://www.coseti.org/natsolar.htm>

Table 2. Atmospheric parameters for the analysed stars of the Praesepe cluster. Columns two to five show the fundamental parameters derived from Strömgren and Geneva photometry. The sixth and seventh columns show the final adopted parameters derived from spectroscopy. The errors on the fundamental parameters are estimated to be 200 K, 0.7 km s⁻¹ and 0.2 dex for T_{eff} , v_{mic} and $\log g$ respectively. The estimated error on $v \sin i$ is about 5%. v_r is given in km s⁻¹. The uncertainty in v_r depends strongly on the $v \sin i$. For a low $v \sin i$ value the error bar on v_r is estimated to be about 1 km s⁻¹, that increases till about 8 km s⁻¹ for the faster rotators.

HD	Strömgren photometry		Geneva photometry		final set			v_{mic} [km s ⁻¹]	$v \sin i$ [km s ⁻¹]	$\sigma_{v \sin i}$ [km s ⁻¹]	v_r [km s ⁻¹]	σ_{v_r} [km s ⁻¹]
	T_{eff} [K]	$\log g$ [cgs]	T_{eff} [K]	$\log g$ [cgs]	T_{eff} [K]	$\log g$ [cgs]	T_{eff} [K]					
72757	7330	3.81			7400	3.60	2.7	179	10	35.8	7.0	
72846	8187	3.85	8146	4.12	8045	3.50	2.5	119	6	35.1	7.3	
73175	7735	3.94	7506	4.22	7660	3.94	2.6	163	9	36.7	5.7	
73345	7779	3.92	7865	4.43	7993	3.96	2.6	85	4	34.5	4.4	
73450	7271	3.77	7455	4.26	7270	4.20	2.7	138	7	34.5	5.1	
73574	7659	3.90	7733	4.36	7662	4.00	2.6	102	4	35.3	4.5	
73746	7390	4.01	7236	4.16	7440	4.08	2.7	95	4	34.2	3.6	
73798	7355	3.80	7301	4.11	7328	3.95	2.7	200	11	34.1	5.9	
73993	7124	3.74	7153	4.11	7138	3.92	2.8	240	14	33.6	7.5	
74028	7517	3.65	7772	4.34	7750	4.50	2.6	150	9	35.3	7.4	
74050	7767	3.78	7722	4.19	7872	3.66	2.6	188	8	36.0	7.8	
74135			7016	4.22	7400	4.00	2.7	100	4	32.5	5.7	
74587			7246	4.15	7500	4.20	2.7	90	4	33.9	4.1	
74589	7581	4.04			7550	4.03	2.7	127	5	34.1	4.7	
74656			7517	4.11	7800	3.99	3.6	25	1	34.1	1.3	
74718	7599	3.99	7453	4.21	7600	4.00	2.7	155	7	34.1	5.7	

and $\log g$ by ± 200 K and ± 0.2 dex respectively. Our tests show that the spectroscopic parameters are comparable or better than the photometric parameters. Furthermore, the tests show a variation of less than 0.2 dex in abundance due to the temperature variation. No significant abundance change was found varying when $\log g$. However, the v_{mic} value and its associated uncertainty increase their importance for rapidly rotating stars, and for this reason we have performed the following additional test. For four stars with different $v \sin i$ values (HD 73730, $v \sin i = 29$ km s⁻¹– HD 73746, $v \sin i = 95$ km s⁻¹– HD 72757, $v \sin i = 179$ km s⁻¹– HD 73798, $v \sin i = 200$ km s⁻¹) we have performed the abundance analysis of selected Fe, Ni, Cr and Ti lines for assumed v_{mic} varying from 1 to 5 km s⁻¹ in steps of 0.1 km s⁻¹. We have then plotted in Fig. 3 and in Fig. 4 the variation of the standard deviation from the mean abundance (upper panel) and the mean abundance itself (lower panel) as a function of v_{mic} .

Figures 3 and 4 show that the adopted v_{mic} value (2.7 km s⁻¹ for all the stars taken into account in this test) obtained with Eq. 1 is reasonable at every rotational velocity. The only exception is for the Am stars, for which slightly larger values of v_{mic} are obtained for those stars for which this quantity is directly derived. Taking into account the different best v_{mic} values obtained from different elements, and the dispersion of the standard deviation as a function of v_{mic} , the uncertainty that we assign to v_{mic} , for the rapid rotators, is 0.7 km s⁻¹. The lower panels of Fig. 3 and Fig. 4 allow us to derive directly the abundance uncertainty given the uncertainty of v_{mic} for each element. We have used Fe as a standard element to derive the abundance standard error, since it is the element with the highest number of selected lines. An error bar of 0.7 km s⁻¹ in v_{mic} produces an uncertainty of element abundance increasing from 0.1 dex for the slow rotators, to 0.2 dex for the rapid rotators. The error bar on the element abundance is dominated by the uncertainty of T_{eff} for the slow rotators, while the uncertainty in v_{mic} becomes increasingly important for larger $v \sin i$. Assuming that T_{eff} and v_{mic} are completely uncorrelated, the resultant abundance error bar for the rapidly rotating stars is given by standard error prop-

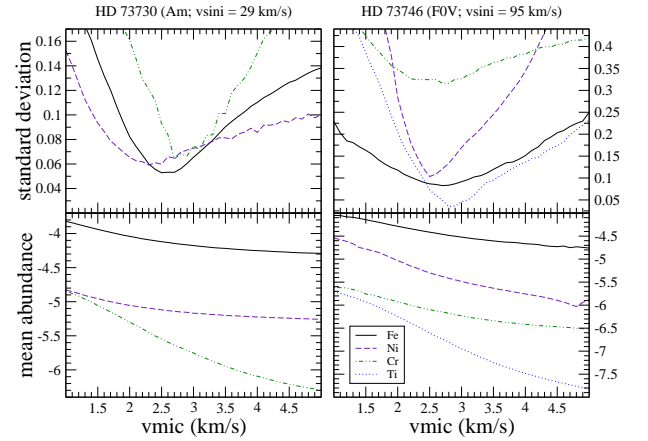


Fig. 3. The upper panels show the variation of the standard deviation from the mean abundance of Fe, Ni, Cr and Ti as a function of v_{mic} , for HD 73730 ($v \sin i = 29$ km s⁻¹) and HD 73746 ($v \sin i = 95$ km s⁻¹). The lower panels show the variation of the mean abundance as a function of v_{mic} .

agation theory, which leads to an uncertainty of about 0.3 dex. In conformity with this analysis, we assume an abundance error bar increasing linearly with $v \sin i$ from 0.2 dex to 0.3 dex at a $v \sin i$ value of 200 km s⁻¹.

Another source of uncertainty that is dependent on $v \sin i$ is due to the continuum normalisation. To quantify this uncertainty we have performed the following test. We have derived the abundance of the Fe II line at 5325.6 Å for HD 73746 ($v \sin i = 95$ km s⁻¹), HD 72757 ($v \sin i = 179$ km s⁻¹) and HD 73798 ($v \sin i = 200$ km s⁻¹) with the adopted normalised observed spectrum and with the spectrum multiplied/divided by 0.99. In this way we

Table 3. Abundances ($\log(N_X/N_{tot})$) of the program stars with the estimated internal errors in units of 0.01 dex, in parenthesis. The internal error associated with the derived abundance of each element is the standard deviation from the mean abundance of the selected lines of that element. For comparison, the solar abundances (Asplund et al. 2005) are given in the last column. At.N. gives the Atomic Numbers of the elements. Abundances obtained from just one line have no error (-;1). Upper limits are denoted by <. The second number in the brackets is the number of lines used to derive the mean abundance.

At.N.	Element	"Normal" A-type stars								Solar Abundances	
		HD 72846	HD 73345	HD 73450	HD 73574	HD 74028	HD 74050	HD 74587	HD 74718		
3	Li	< -8.08(-; 1)	< -8.33(-; 1)	< -8.70(-; 1)	< -8.38(-; 1)			< -8.41(-; 1)	< -8.26(-; 1)	-10.99	
6	C	-3.58(-; 1)	-3.44(12; 3)	-3.27(-; 1)	-3.36(18; 2)	-3.39(08; 2)	-3.52(-; 1)	-3.49(01; 2)	-3.51(04; 2)	-3.65	
8	O	-3.18(-; 1)	-3.22(01; 2)				-3.70(-; 1)	-3.30(-; 1)		-3.38	
11	Na	-5.44(01; 2)	-5.37(01; 2)	-6.28(-; 1)	-5.57(02; 2)	-5.98(-; 1)	-5.64(13; 2)	-5.61(02; 2)	-5.70(14; 2)	-5.87	
12	Mg	-4.18(08; 3)	-4.18(02; 3)	-5.02(18; 2)	-4.37(04; 3)	-4.86(08; 3)	-4.22(05; 4)	-4.56(08; 3)	-4.52(01; 2)	-4.51	
14	Si	-4.62(16; 2)	-4.67(-; 1)	-4.13(-; 1)	-4.19(-; 1)	-4.17(-; 1)	-4.37(-; 1)	-4.16(-; 1)	-4.25(-; 1)	-4.53	
16	S	-4.71(04; 2)	-4.44(03; 4)	-4.35(-; 1)	-4.61(02; 2)	-4.26(01; 2)		-4.50(04; 2)	-4.28(11; 2)	-4.90	
20	Ca	-5.17(-; 1)	-5.39(09; 6)	-5.95(06; 4)	-5.86(16; 5)	-5.37(16; 2)	-6.13(06; 2)	-5.49(15; 6)	-5.68(02; 3)	-5.73	
21	Sc	-8.88(-; 1)	-8.63(07; 3)	-8.57(14; 3)	-8.89(02; 3)	-8.35(-; 1)	-8.96(27; 3)	-8.56(-; 1)	-8.69(14; 2)	-8.99	
22	Ti	-6.88(03; 5)	-6.95(06; 6)	-7.30(11; 5)	-6.98(09; 5)	-6.78(-; 1)	-7.08(15; 5)	-6.83(16; 3)	-6.93(10; 5)	-7.14	
24	Cr	-6.23(06; 3)	-6.22(08; 2)	-6.56(08; 3)	-6.19(16; 3)	-6.23(12; 4)	-6.48(10; 3)	-6.05(13; 4)	-6.44(20; 5)	-6.40	
25	Mn		-6.37(-; 1)	-6.88(-; 1)	-6.52(02; 2)	-6.77(-; 1)	-6.61(-; 1)	-6.62(04; 2)	-6.71(-; 1)	-6.65	
26	Fe	-4.55(18; 42)	-4.33(11; 61)	-4.62(09; 15)	-4.49(10; 30)	-4.50(09; 18)	-4.44(13; 16)	-4.28(10; 33)	-4.61(11; 26)	-4.59	
28	Ni	-5.70(18; 2)	-5.58(11; 4)	-5.82(16; 2)	-5.62(08; 4)	-5.93(14; 3)	-5.60(15; 3)	-5.84(-; 1)	-5.68(02; 3)	-5.81	
39	Y	-9.75(-; 1)	-9.46(-; 1)	-9.83(-; 1)	-9.20(-; 1)	-9.56(-; 1)	-9.26(-; 1)	-9.13(-; 1)	-9.10(-; 1)	-9.83	
56	Ba	-9.48(-; 1)	-9.30(06; 2)	-9.50(02; 2)	-8.98(04; 2)	-9.65(-; 1)	-9.52(01; 2)	-8.96(25; 2)	-9.15(-; 1)	-9.87	
	T_{eff}	8045	7993	7270	7662	7750	7872	7500	7600		
	$\log g$	3.50	3.96	4.20	4.00	4.50	3.66	4.20	4.00		
	v_{mic}	2.5	2.6	2.7	2.6	2.6	2.6	2.7	2.7		
	$v \sin i$	119	85	138	102	150	188	90	155		
At.N.	Element	F-type stars							Am star HD 74656	Solar Abundances	
		HD 72757	HD 73175	HD 73746	HD 73798	HD 73993	HD 74135	HD 74589			
3	Li			< -8.70(-; 1)				< -8.47(-; 1)	< -8.35(-; 1)	-8.61(-; 1)	-10.99
6	C	-3.71(16; 2)	-3.36(01; 2)	-3.39(-; 1)				-3.30(14; 2)	-3.19(18; 2)	-4.09(-; 1)	-3.65
7	N									-3.98(-; 1)	-4.26
8	O			-3.30(-; 1)				-3.40(-; 1)	-3.36(-; 1)	-3.88(-; 1)	-3.38
11	Na	-5.61(-; 1)	-5.81(01; 2)	-5.45(13; 2)				-5.73(24; 2)	-5.73(07; 2)	-5.35(01; 2)	-5.87
12	Mg	-4.56(14; 2)	-4.38(07; 2)	-4.50(11; 5)	-4.76(23; 2)	-4.57(-; 1)		-4.14(09; 2)	-4.25(02; 2)	-4.73(11; 3)	-4.51
13	Al									-5.15(-; 1)	-5.67
14	Si	-4.23(06; 3)	-4.39(-; 1)	-4.29(-; 1)	-4.09(-; 1)	-4.34(-; 1)		-4.14(-; 1)	-4.20(-; 1)	-4.37(-; 1)	-4.53
16	S	-4.62(01; 2)	-4.55(-; 1)	-4.54(05; 5)				-4.62(05; 2)	-4.44(07; 2)	-4.52(04; 5)	-4.90
20	Ca	-5.60(11; 6)	-5.41(03; 3)	-5.68(16; 8)	-5.38(15; 5)	-5.65(-; 1)		-5.45(14; 4)	-5.53(05; 7)	-6.34(13; 3)	-5.73
21	Sc	-9.07(-; 1)	-8.66(-; 1)	-8.98(10; 3)	-9.20(-; 1)	-8.90(-; 1)		-8.48(15; 4)	-8.43(25; 3)	-9.27(-; 1)	-8.99
22	Ti	-7.03(16; 5)	-6.90(15; 3)	-6.68(13; 3)	-6.90(-; 1)	-7.18(-; 1)		-7.03(09; 6)	-6.92(11; 7)	-6.90(16; 18)	-7.14
23	V									-7.06(-; 1)	-8.04
24	Cr	-6.72(08; 3)	-6.55(01; 2)	-6.20(23; 6)	-6.64(36; 4)			-6.16(12; 3)	-6.26(20; 4)	-5.72(10; 11)	-6.40
25	Mn	-6.92(-; 1)	-6.98(08; 2)	-6.46(01; 2)	-6.36(-; 1)			-6.42(11; 3)		-6.27(11; 5)	-6.65
26	Fe	-4.50(08; 31)	-4.52(08; 14)	-4.46(08; 49)	-4.47(06; 17)	-4.47(08; 6)		-4.45(11; 60)	-4.51(11; 53)	-4.11(13; 74)	-4.59
27	Co									-5.38(-; 1)	-7.12
28	Ni	-5.57(-; 1)	-5.68(05; 3)	-5.38(12; 5)	-6.20(07; 2)	-6.15(-; 1)		-5.53(10; 4)	-5.90(17; 4)	-5.00(08; 15)	-5.81
29	Cu									-6.92(-; 1)	-7.83
30	Zn									-6.77(-; 1)	-7.44
38	Sr									-8.23(-; 1)	-9.12
39	Y	-10.07(-; 1)	-9.39(-; 1)	-9.35(01; 2)	-9.20(-; 1)			-9.46(-; 1)	-8.99(-; 1)	-8.92(11; 3)	-9.83
40	Zr									-8.62(-; 1)	-9.45
56	Ba	-9.12(06; 2)	-9.64(-; 1)	-9.02(12; 2)	-8.78(-; 1)	-9.48(-; 1)		-9.10(-; 1)	-9.14(-; 1)	-8.46(23; 3)	-9.87
57	La									-9.22(14; 3)	-10.91
58	Ce									-9.11(08; 3)	-10.46
60	Nd									-9.27(13; 5)	-10.59
62	Sm									-9.89(-; 1)	-11.03
63	Eu									-9.89(-; 1)	-11.52
68	Er									-9.53(-; 1)	-11.11
70	Yb									-9.46(-; 1)	-10.96
	T_{eff}	7400	7660	7440	7328	7138	7400	7550	7800		
	$\log g$	3.60	3.94	4.08	3.95	3.92	4.00	4.03	3.99		
	v_{mic}	2.7	2.6	2.7	2.7	2.8	2.7	2.7	3.6		
	$v \sin i$	179	163	95	200	240	100	127	25		

have increased/decreased the continuum level of 1%, that we estimate to be a reasonable uncertainty. The difference between the abundances obtained in this way is increasing with $v \sin i$ from about 0.1 dex for HD 73746, to about 0.2 dex for the two faster rotators. We believe that in most cases this error bar is an upper limit since the line by line abundance analysis method, used in this work, allows a very careful line selection that rejects all the lines for which the continuum level looks uncertain. Under the assumption of no systematic errors in the continuum normalisation, this uncertainty is decreasing with an increase of the number of selected lines. If for some lines the continuum level is too low, for some others it would be too high, leading to an increase of the dispersion, but not to an abundance variation.

An example of the spectrum of a rapidly rotating star and the synthetic spectrum obtained after the complete abundance analysis is shown in Fig. 16 (available online).

For all the rapid rotators in our sample, we were able to obtain only an upper limit on the abundance of Li, because the high $v \sin i$ values did not allow us to detect the Li line. Only the Li abundance of HD 74656 may be considered as a real estimate, although even this value is uncertain because it was derived only from one blended line.

We confirm the membership in Praesepe of all the stars of our sample, because the v_t measurements are all compatible with the cluster mean of $34.5 \pm 0.0 \text{ km s}^{-1}$ (Robichon et al. 1999). For none of the analysed stars have we found any evidence of bina-

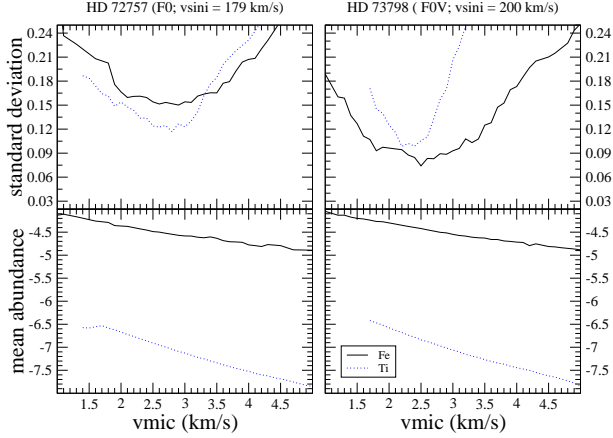


Fig. 4. As for Fig. 3, but for HD 72757 ($v \sin i = 179 \text{ km s}^{-1}$) and HD 73798 ($v \sin i = 200 \text{ km s}^{-1}$).

rity. These considerations confirm the quality of our target selection (which were selected for membership and non-binarity).

We confirm the Am classification of HD 74656. In Fig. 15 (available online) the mean abundances for the Am stars analysed in Paper I are compared with the abundances obtained for HD 74656. The comparison shows a good agreement between the two abundance patterns.

6. Discussion

In this section we discuss the results obtained considering both samples of stars: those analysed in this work, and those from Paper I. In the sample of stars from Paper I, we have not included results for HD 73666 (Blue Straggler), HD 72942 (probable non-member) and HD 73174, for which the derived T_{eff} from Strömgen photometry and from spectroscopy differ by about 700 K and no explanation was found in Paper I. For this reason we have decided not to consider this object in our final analysis of the cluster.

6.1. Abundances of the A- and F-type stars of the Praesepe cluster

The stars were first grouped according to their classifications as F, A and Am stars; Fig. 5 shows the mean abundances for each group. The error bars in Fig. 5 are the standard deviations from the calculated mean abundances of each group.

The A- and F-type stars show similar abundance patterns, characterised by solar abundances for almost all the elements. The Am stars show the typical abundance pattern characterised by underabundances of C, N, O, Ca and Sc, with a general overabundance of the other elements. As expected, the error bars associated with the abundances of the F-type stars turn out to be comparable to or smaller than those for the A-type stars. It is also possible to see this effect in Figures from 7 to 9.

We have calculated the metallicity of the cluster (Z) from the abundances derived for the F-type stars, excluding HD 73575. This star is close to the TAMS and its Fe abundance differs by 0.27 dex with respect to the mean Fe abundance (0.11 ± 0.03 dex) of the other F-type stars. For this reason we have omit-

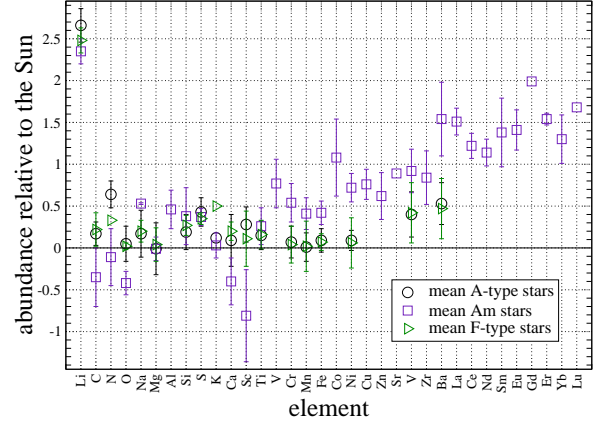


Fig. 5. Comparison between the mean abundances obtained for Am, A- and F-type stars indicated by an open circle, square and triangle respectively. The error bars are the standard deviations from the calculated mean abundances. In the case of only one measurement, no error bar is shown. A- and F-type stars show a similar abundance pattern. The Am stars show the typical peculiar abundance pattern described in detail in Paper I.

ted HD 73575 from the determination of the cluster metallicity. The Z value we obtain is 0.015 ± 0.002 dex.

The Z value adopted by several other authors and used to characterise isochrones (see Sect. 6.2) is calculated with the following approximation:

$$Z_{\text{cluster}} \simeq 10^{([Fe/H]_{\text{stars}} - [Fe/H]_{\odot})} \cdot Z_{\odot}, \quad (2)$$

assuming $Z_{\odot} = 0.019$ dex. We have recalculated the Z of the cluster according to this approximation obtaining $Z = 0.024 \pm 0.02$. We have derived this value using the mean Fe abundance of all the F-type stars except HD 73575 ($[Fe/H] = 0.11 \pm 0.03$ dex).

Our estimated metallicity is in agreement with that included in the catalogue of Chen et al. (2003) of $[Fe/H] = 0.14$ dex and with that recently obtained by An et al. (2007) of $[Fe/H] = 0.11 \pm 0.03$ dex. An et al. (2007) derived the metallicity from an Fe abundance determination from high resolution spectra of four G-type cluster members.

6.2. HR diagram

Using the spectroscopic temperatures determined to perform the abundance analysis we have built the Hertzsprung–Russell (HR) diagram of the cluster around the turn-off point (Fig. 6). We have calculated the luminosity of each star photometrically, adopting the magnitudes in V band given by SIMBAD and a cluster distance modulus of 6.30 ± 0.07 mag (van Leeuwen 2007). We have used a reddening of 0.009 mag (WEBDA) and the bolometric correction given by Balona (1994). Luminosities are listed in Table 4. With a distance modulus uncertainty of 0.07 mag, an uncertainty in the bolometric correction of about 0.07 mag, and a reddening uncertainty of 0.01 mag, we estimate that the typical uncertainty in M_{bol} is about 0.15 mag, corresponding to an uncertainty in $\log L/L_{\odot}$ of about 0.06 dex.

In the diagram we have divided our sample into Am stars (crosses) and normal A- and F-type stars (full squares). We have

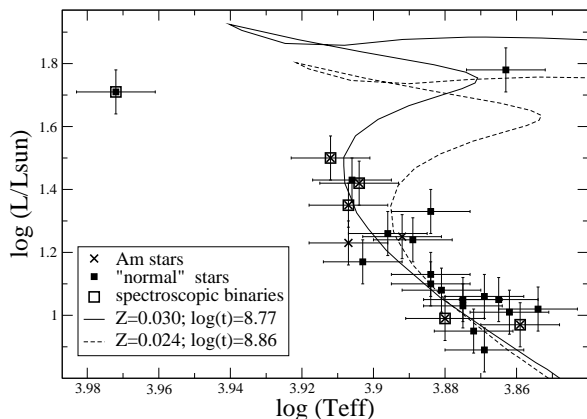


Fig. 6. Hertzsprung–Russell diagram of the Praesepe cluster. The crosses and filled squares show the position on the HR diagram for the Am and normal A- and F-type stars, respectively. The open squares indicate the spectroscopic binaries. We have not corrected the luminosities of these stars due to the presence of a companion, but we assume it less than 0.1 dex. The error bar in luminosity is 0.07 dex. The dashed line shows an isochrone from Girardi et al. (2002) for the age and metallicity given in the literature ($\log t = 8.85$ dex; $Z = 0.024$ dex). The solid line shows the isochrone corresponding to our best fit ($\log t = 8.77$ dex; $Z = 0.030$ dex).

also denoted (open squares) the spectroscopic binary stars. We have not corrected the luminosities of the spectroscopic binaries, as the only information we have about the secondaries is that their contribution to the analysed spectra is not detected (Paper I). This suggests that their flux contribution is below about 5%.

The two stars located at the top left and top right of the HR diagram are HD 73666 and HD 73575, respectively. Both have already been analysed in detail in Paper I. HD 73666 is clearly a Blue Straggler, while HD 73575 should be just at the TAMS, if the stars are cluster members (membership given by HIPPARCOS and confirmed in Paper I). HD 73575 deserves a further comment. It is the most evolved star of the cluster and the position close to the TAMS is consistent with this. This star also shows anomalous chemical composition compared with that of the other normal F-type stars. The position on the HR diagram and the peculiar chemical composition of HD 73575 suggest an unusual evolutionary history.

We have adopted isochrones by Girardi et al. (2002) to determine age and metallicity of the cluster using the HR diagram. In Fig. 6 we have plotted two isochrones: one corresponding to the age and metallicity of the cluster taken from WEBDA ($\log t = 8.85$ dex; $Z = 0.024$ dex; dashed line) and the other corresponding to our best fit on the HR diagram ($\log t = 8.77$ dex; $Z = 0.030$ dex; solid line).

An et al. (2007) determined the metallicity of the Praesepe cluster by fitting Yale Rotating Evolutionary Code (YREC, Sills et al. 2000) isochrones to the main sequence of the cluster, obtained from Johnson photometry. They derived a metallicity of $[\text{Fe}/\text{H}] = 0.20 \pm 0.04$ corresponding to $Z = 0.030 \pm 0.003$. This re-

sult is in agreement with the results of our fits of isochrones to our sample of stars around the turn-off point.

All the Am stars are on the main sequence. Only HD 73618 (the hottest main sequence star in Fig. 6) can be considered a Blue Straggler (Ahumada & Lapasset 2007), taking into account the age and metallicity given in the literature.

6.3. Abundances vs. T_{eff} and $v \sin i$

The abundances of the elements analysed for most of the stars are displayed against T_{eff} and $v \sin i$ in the left and right panels respectively from Fig. 7 to Fig. 9. We have divided the sample of stars according to their spectral classification: A-type stars (open circles), Am stars (open squares) and F-type stars (open triangles). This division and visualisation will be retained in the following sections.

The plots show that the abundances of the F-type stars are less scattered than those obtained for the A-type stars, as expected.

For the normal A- and F-type stars we do not find any clear correlation between abundance and T_{eff} or abundance and $v \sin i$. This result confirms the prediction of Charbonneau & Michaud (1991).

For the Am stars, none of the plotted elements, except Y, shows any trend between abundance and T_{eff} . Richer et al. (2000) predict mild correlations between abundances of some elements (e.g. Ni) and T_{eff} , but probably our temperature range is not large enough to show such correlations.

In Am stars, we find a strong correlation between abundance and $v \sin i$ for all peculiar elements, except for scandium and titanium. As described in detail in Paper I, Am stars of the Praesepe cluster show peculiarities mainly for C, O, Ca and Sc (underabundant) and Ti, Cr, Fe, Ni, Y and Ba (overabundant). C, O and Ca show an increasing abundance with $v \sin i$. The Fe-peak elements, Y, and Ba show a decreasing abundance with $v \sin i$. Na, Mg, Si and S are not peculiar in Am stars and they do not show any correlation with $v \sin i$. As a general behavior, the peculiarities decrease with $v \sin i$, becoming closer and closer to the abundances typical of the normal A- and F-type stars of the cluster. Scandium and titanium are exceptions: Ti does not show any clear trend with $v \sin i$, and Sc shows a trend opposite to that of C, O and Ca, while we would have expected a similar behavior.

Burkhart (1979) derived the abundance anomaly, from the Strömgren m_1 index, and $v \sin i$ values for a sample of well-known Am stars. She suggested a jump in the abundance anomaly for stars with $v \sin i > 55 \text{ km s}^{-1}$; our results confirm this claim.

Models by Charbonneau & Michaud (1991) do not predict any strong correlation between element abundances and rotational velocity: "For FmAm stars, it was shown quantitatively that despite the potentially inhibiting effects of meridional circulation on chemical separation, no dependence of abundance anomalies on $v \sin i$ is expected, for most elements, in the rotational velocity interval characteristic of FmAm stars." The correlations here obtained between abundance and $v \sin i$, for the Am stars, are in clear disagreement with the predictions of Charbonneau & Michaud (1991).

Richer et al. (2000) found that element abundances in model Am stars are dependent only on the depth of the zone mixed by turbulence, thus showing that the abundance anomalies in Am stars depend mainly on the turbulence model.

More recently, Talon et al. (2006) tested rotational mixing models with both the Geneva–Toulouse and Montreal codes.

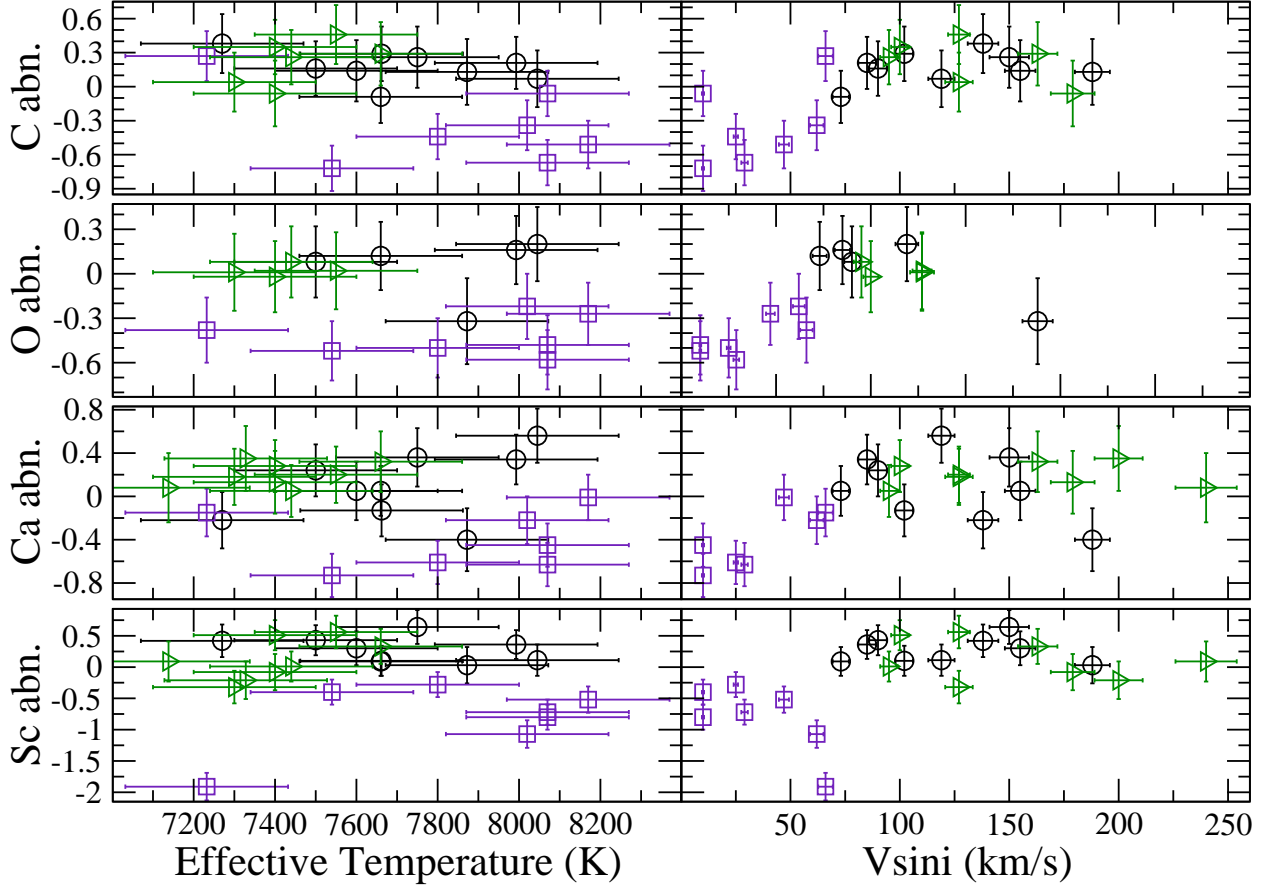


Fig. 7. Abundances relative to the Sun (Asplund et al. 2005) of C, O, Ca and Sc as a function of T_{eff} and $v \sin i$ for normal A-type stars (circle), Am stars (square) and normal F-type stars (triangle). A correlation between abundances of C, O, Ca and $v \sin i$ is found for Am stars; an anticorrelation between Sc abundance and $v \sin i$ is found for Am stars.

They showed how the predicted surface abundances of FmAm stars should vary as a function of rotational velocity of the star. Our findings support their predictions.

6.4. Abundances vs. M/M_{\odot} and fractional age

For the stars in our sample we have calculated M/M_{\odot} , fractional age (τ) and their uncertainties according to Landstreet et al. (2007) and listed them in Table 4.

We have taken the abundances of three representative elements (Mg, Ca and Fe) showing, for the Am stars, the three different properties discussed in Sect. 6.3. We plot the abundances of these elements as functions of M/M_{\odot} and display the results in Fig. 10.

No clear correlation is visible for any of the three plotted elements, for the normal or the Am stars.

Richer et al. (2000) suggest that the abundance anomalies typical of Am stars depend very little on the mass and therefore

fractional age of the star. This is consistent with the results of this study.

6.5. Searching for correlations between abundances

In a sample of seventeen Am stars, Adelman & Unsuere (2007) found significant correlations between the abundances of twelve elements.

The abundances of the elements analysed in most of the stars of our sample are displayed against the Fe abundance in Fig. 11 and Fig. 12.

We do not find any clear correlation between the abundances of any element and Fe for the A- and F-type stars due to the tiny spread in Fe abundance.

In contrast, the Am stars show correlations for all the elements in which a correlation was already found with $v \sin i$. The Fe abundance is an indicator of Am peculiarities. As we have

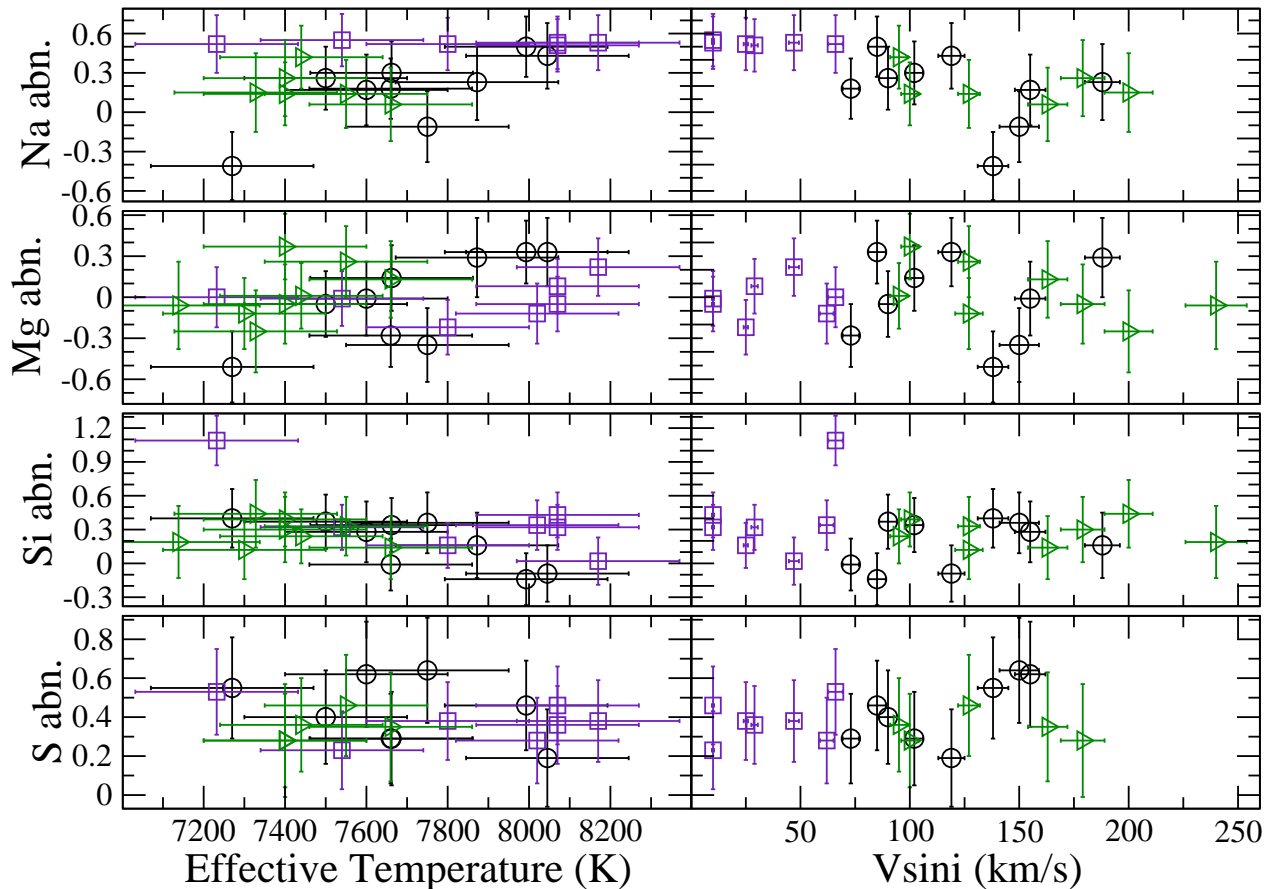


Fig. 8. Same as in Fig. 7 but for Na, Mg, Si and S. No correlation is found.

found a correlation between $\nu \sin i$ and Am peculiarities, it is not surprising to obtain similar correlations with the Fe abundance.

The correlations found for C and O are in agreement with those found by Savanov (1995) in a sample of seventeen well-known Am stars analysed by different authors. They looked for a correlation between the C abundance and $\nu \sin i$, but without any positive result.

From our results it is clear that these correlations are related to those found with $\nu \sin i$ in Sect. 6.3.

7. Conclusions

We have obtained high resolution, high SNR spectra for seventeen F- and A-type stars of the Praesepe open cluster, with the SOPHIE spectrograph at OHP. One of these stars (HD 74656) was classified as Am star.

We have calculated the fundamental parameters and performed a detailed abundance analysis for all the stars of the sample, confirming the previous classification, as chemically peculiar, of the Am star HD 74656.

The stars we observed were selected using a standard procedure that will be adopted for future analysis of other open clusters. All the selected stars of the sample shown in Table 1 are confirmed members of the cluster and among them there are no known binaries (except HD 73666). This shows the quality of the selection procedure, since membership and non-binarity were required for the selection.

To be able to discuss general properties of the cluster we have added to our sample of stars those considered in Paper I. Of the stars analysed in Paper I we have not included HD 73666 (Blue Straggler), HD 72942 (not a confirmed member) and HD 73174 (important uncertainties in T_{eff}). The sample of stars analysed in Paper I and in this work contains all the known cluster members with a spectral type between F2 and A1 and not SB2. This removes any bias that could have been introduced by an inappropriate target selection.

We have divided our final sample of stars according to their spectral classification, taken from WEBDA, and derived the mean abundance pattern for three groups of stars: A-, F-type and Am. The A- and F-type stars show a similar abundance

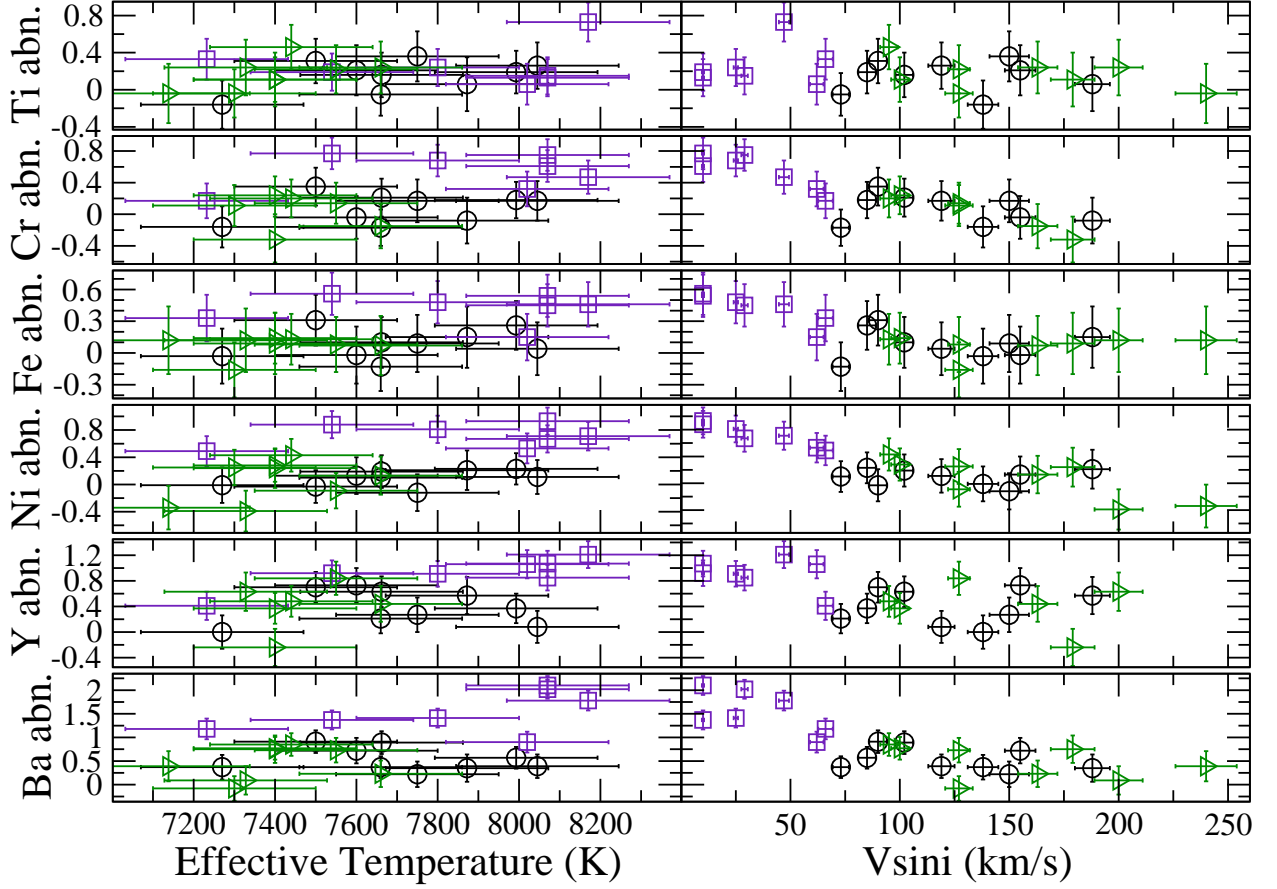


Fig. 9. Same as in Fig. 7 but for Ti, Cr, Fe, Ni, Y and Ba. No correlation is found for Ti. An anticorrelation between Cr, Fe, Ni, Y and Ba abundance and $v \sin i$ is found for Am stars.

pattern, close to solar, while the Am stars show the typical Am peculiarities described in Paper I. The abundance scatter of the Am stars is higher than for the normal stars and, between A- and F-type stars, the F-stars show the smaller scatter, as expected.

We have derived the metallicity of the cluster from the F-type stars of our sample, omitting HD 73575 which is already on the TAMS. The resultant metallicity is $Z = 0.015 \pm 0.002$ dex. To be able to compare our metallicity ($[Fe/H] = 0.11 \pm 0.03$) with that used by other authors we have derived Z with the approximation given by Eq. 2 that corresponds to $Z = 0.024 \pm 0.002$ dex, assuming $Z_{\odot} = 0.019$ dex. This result is in agreement with previous metallicity determinations from abundance analysis of G-type stars by An et al. (2007).

For each star of the sample we have photometrically derived $\log L/L_{\odot}$ and, adopting the spectroscopic temperatures derived for the abundance analysis, built the Hertzsprung–Russell (HR) diagram of the cluster around the turn-off point. We have fitted isochrones by Girardi et al. (2002) to our HR diagram to derive age and metallicity ($\log t = 8.77 \pm 0.1$ dex; $Z = 0.030 \pm 0.007$

dex). This result is in agreement with that obtained by An et al. (2007) fitting YREC isochrones to a photometrically-derived main sequence of the cluster. We confirm the discrepancy in metallicity found by An et al. (2007). Within the errors, our age determination agrees with earlier determinations in the literature ($\log t = 8.85 \pm 0.15$, González-García et al. 2006).

We have plotted the abundances of the elements analysed in most of the stars of our sample as a function of T_{eff} and $v \sin i$. We have not found any clear abundance trend with respect to T_{eff} and $v \sin i$ for the A- and F-type stars. However, we have found several trends between abundances and $v \sin i$ for Am stars. Correlations are present for the elements that characterise the Am peculiarities. Only Sc and Ti do not show this trend. With increasing $v \sin i$ the peculiarities tend to weaken, and the abundances approach the mean of the other A- and F-type stars. This is the first real observational evidence of a direct connection between abundance anomalies or diffusion processes and rotational velocity in Am stars.

Table 4. $\log L/L_{\odot}$, $\log T_{\text{eff}}$, M/M_{\odot} and fractional age (τ) with associated error bars for the analysed stars of the Praesepe cluster. The error bar in luminosity is ~ 0.06 dex, as explained in Sect. 6.2. No fractional age is given for HD 73666 since it is a Blue Straggler.

HD	$\log L/L_{\odot}$ dex	Sp.Type	$\log T_{\text{eff}}$	M/M_{\odot}	$\sigma_{M/M_{\odot}}$	τ	σ_{τ}
72757	1.06	F0	3.869	1.71	0.09	0.43	0.06
72846	1.43	A5V	3.906	2.09	0.15	0.76	0.11
73045	0.99	Am	3.880	1.67	0.08	0.40	0.06
73175	1.13	F0V	3.884	1.78	0.09	0.48	0.07
73345	1.17	A7V	3.903	1.84	0.13	0.53	0.08
73430	1.10	A7V	3.884	1.76	0.09	0.47	0.07
73450	1.01	A9V	3.862	1.66	0.08	0.39	0.06
73574	1.33	A8V	3.884	1.96	0.10	0.64	0.10
73575	1.78	F0III	3.863	2.33	0.12	1.02	0.15
73618	1.50	Am	3.912	2.16	0.22	0.84	0.13
73666	1.71	A0	3.972	2.46	0.12	0.12	0.18
73709	1.35	Am	3.907	2.00	0.14	0.68	0.10
73711	1.42	Am	3.904	2.08	0.10	0.75	0.11
73730	1.23	Am	3.907	1.89	0.13	0.58	0.09
73746	0.95	F0V	3.872	1.64	0.08	0.38	0.06
73798	1.05	F0V	3.865	1.70	0.12	0.42	0.06
73818	0.97	Am	3.859	1.63	0.08	0.37	0.06
73993	1.02	F2V	3.854	1.66	0.12	0.39	0.06
74028	1.24	A7V	3.889	1.88	0.09	0.57	0.09
74050	1.26	A6V	3.896	1.91	0.10	0.60	0.09
74135	0.89	F0	3.869	1.60	0.08	0.35	0.05
74587	1.03	A5	3.875	1.71	0.09	0.43	0.06
74589	1.05	F0	3.875	1.70	0.09	0.42	0.06
74656	1.25	Am	3.892	1.89	0.09	0.58	0.09
74718	1.08	A5	3.881	1.74	0.09	0.45	0.07

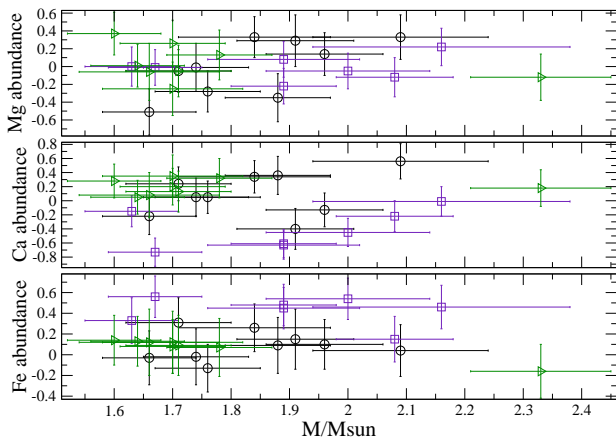


Fig. 10. Abundances relative to the Sun (Asplund et al. 2005) of Mg, Ca and Fe as a function of the M/M_{\odot} . No correlations are found.

The Praesepe cluster could be peculiar in this sense because it contains a high number of Am stars. This fact, combined with the advanced age of the cluster, makes it possible to have many Am stars close to the turn-off point. Since diffusion is a slow process, in this cluster, more than in others, the peculiarities are evident and well-characterised by correlations between abundance anomalies and rotational velocity. Similar relationships may be less obvious in younger clusters. It will clearly be of interest to check this possibility.

The trends obtained in this work are in disagreement with those predicted by Charbonneau & Michaud (1991), as accord-

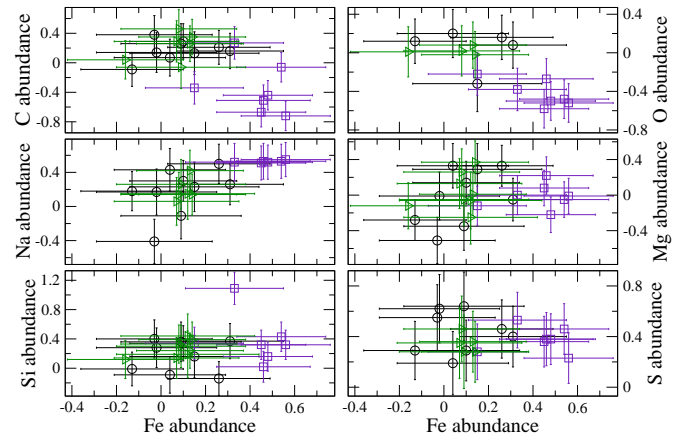


Fig. 11. Abundances relative to the Sun (Asplund et al. 2005) of C, O, Na, Mg, S and Si as a function of the Fe abundance.

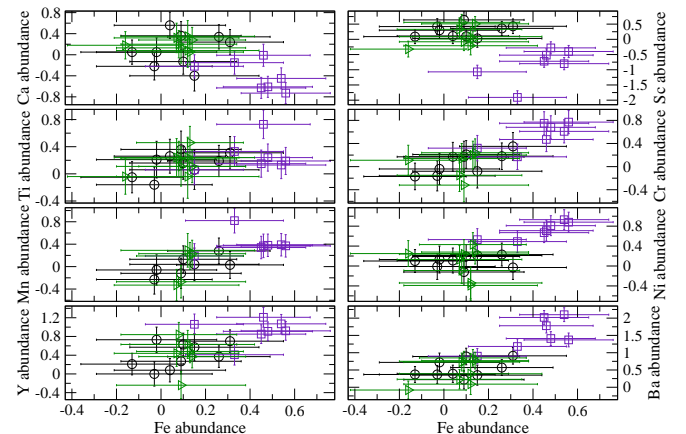


Fig. 12. Same as in Fig. 11 but for Ca, Sc, Ti, Cr, Mn, Ni, Y and Ba.

ing to their models meridional circulation does not affect abundance peculiarities. Recently Richer et al. (2000) and later Talon et al. (2006) have calculated diffusion models with a more accurate treatment of the rotational mixing. Their predicted abundances for stars with various rotational velocities are qualitatively in agreement with observed properties of our sample of Am stars. Detailed models, with a full treatment of diffusion and rotational mixing, calculated individually for each Am star of our sample, would be necessary for a more substantial comparison between models and observed abundances.

We have derived M/M_{\odot} and fractional age (τ) for each of the stars of our sample and plotted the abundances as a function of M/M_{\odot} . No correlation was found for any of the three spectral groups considered here, as predicted by Richer et al. (2000).

We have searched for correlations between abundances of the elements analysed in most of the stars and the Fe abundance.

For normal A– and F–type stars we have not found any correlation, while for Am stars strong correlations are obtained for all the peculiar elements. The behavior of the abundances of the elements which are peculiar in Am stars, as a function of the Fe abundance, is the same as that found for $\nu \sin i$. We conclude that there is a strong connection between the correlations among the abundances, with the correlations of abundances with $\nu \sin i$.

Acknowledgements. We thank Tanya Ryabchikova for important help and advice given during this investigation. LF and OK have received support from the Austrian Science Foundation (FWF project P17890-N2). JDL and GAW acknowledge support from the Natural Science and Engineering Council of Canada (NSERC). GAW acknowledges support from the Department of National Defence Academic Research Programme (DND-ARP). This paper is based on observations obtained using the SOPHIE spectrograph at the Observatoire de Haute Provence (France). We acknowledge also the OPTICON program (Ref number: 2007/011) for the financial support given to the observing run.

References

- Abt, H. A. 1970, *ApJS*, 19, 387
- Abt, H. A., & Willmarth, D. W. 1999, *ApJ*, 521, 682
- Adelman, S. J., & Unsworth, N. 2007, *Baltic Astronomy*, 16, 183
- Ahumada, J. A., & Lapasset, E. 2007, *A&A*, 463, 789
- An, D., Terndrup, D. M., Pinsonneault, M. H., et al. 2007, *ApJ*, 655, 233
- Asplund, M., Grevesse, N., & Sauval, A. J. 2005, in *ASP Conf. Ser.* 336: Cosmic Abundances as Records of Stellar Evolution and Nucleosynthesis, ed. Thomas G. Barnes III & Frank N. Bash, 25
- Bagnulo, S., Landstreet, J. D., Mason, E., et al. 2006, *A&A*, 450, 777
- Baumgardt, H., Dettbarn, C., & Wielen, R. 2000, *A&AS*, 146, 251
- Balona, L. A. 1994, *MNRAS*, 268, 119
- Burkhart, C. 1979, *A&A*, 74, 38
- Burkhart, C., & Coupry, M. F. 1998, *A&A*, 338, 1073
- Canuto, V. M., & Mazzitelli, I. 1992, *ApJ*, 389, 724
- Charbonneau, P., & Michaud, G. 1991, *ApJ*, 370, 693
- Chen, L., Hou, J. L., & Wang, J. J. 2003, *AJ*, 125, 1397
- Clampitt, L., & Burstein, D. 1997, *AJ*, 114, 699
- Conti, P. S., Hensberge, G., van den Heuvel, E. P. J., & Stickland, D. J. 1974, *A&A*, 34, 393
- Dias, W. S., Assafin, M., Flório, V., Alessi, B. S., & Libero, V. 2006, *A&A*, 446, 949
- Fossati, L., Bagnulo, S., Monier, R., et al. 2007, *A&A*, 476, 911
- Girardi, L., Bertelli, G., Bressan, A., et al. 2002, *A&A*, 391, 195
- Glebocki, R., & Stawikowski, A. 2000, *Acta Astronomica*, 50, 509
- González-Garcá, B. M., Zapatero Osorio, M. R., Béjar, V. J. S., et al. 2006, *A&A*, 460, 799
- Hartkopf, W. I., & McAlister, H. A. 1984, *PASP*, 96, 105
- Hauck, B., & Mermilliod, M. 1998, *A&AS*, 129, 431
- Hill, G. M., & Landstreet, J. D. 1993, *A&A*, 276, 142
- Kharchenko, N. V., Piskunov, A. E., Röser, S., Schilbach, E., & Scholz, R.-D. 2004, *AJ*, 325, 740
- Kochukhov, O. 2006, in *Magnetic Stars*, ed. I. I. Romanyuk, & D. O. Kudryavtsev (in press)
- Kunzli, M., North, P., Kurucz, R. L., & Nicolet, B. 1997, *A&AS*, 122, 51
- Kupka, F., Piskunov, N. E., Ryabchikova, T. A., Stempels, H. C., & Weiss, W. W. 1999, *A&AS*, 138, 119
- Landstreet, J. D., Bagnulo, S., Andretta, V., et al. 2007, *A&A*, 470, 685
- Landstreet, J. D., Silaj, J., Andretta, V., et al. 2007, *A&A*, (in press)
- van Leeuwen, F. 2007, *Hipparcos, the New Reduction of the Raw Data*. Institute of Astronomy, Cambridge University, Cambridge, UK Series: Astrophysics and Space Science Library, Vol. 350 20 Springer Dordrecht
- Madsen, S., Dravins, D., & Lindegren, L. 2002, *A&A*, 381, 446
- Mason, B. D., Hartkopf, W. I., McAlister, H. A., & Sowell, J. R. 1993, *AJ*, 106, 637
- McAlister, H. A., Hartkopf, W. I., Hutter, D. J., & Franz, O. G. 1987, *AJ*, 93, 688
- Mermilliod, J.-C., & Paunzen, E. 2003, *A&A*, 410, 511
- Napiwotzki, R., Schoenberner, D., & Wenske, V. 1993, *A&A*, 268, 653
- Pace, G., Recio-Blanco, A., Piotto, G., & Momany, Y. 2006, *A&A*, 452, 493
- Piskunov, N. E., Kupka, F., Ryabchikova, T. A., Weiss, W. W., & Jeffery, C. S. 1995, *A&AS*, 112, 525
- Pourbaix, D., Tokovinin, A. A., Batten, A. H., et al. 2004, *A&A*, 424, 727
- Renson, P., Gerbaldi, M., & Catalano, F. A. 1991, *A&AS*, 89, 429
- Richer, J., Michaud, G., & Turcotte, S. 2000, *ApJ*, 529, 338
- Robichon, N., Arenou, F., Mermilliod, J.-C., & Turon, C. 1999, *A&A*, 345, 471
- Rodríguez, E., López-González, M. J., & López de Coca, P. 2000, *A&AS*, 144, 469
- Royer, F., Grenier, S., Baylac, M.-O., Gómez, A. E., & Zorec, J. 2002, *A&A*, 393, 897
- Ryabchikova, T. A., Piskunov, N. E., Stempels, H. C., Kupka, F., & Weiss, W. W. 1999, *Phis. Scr.*, T83, 162
- Ryabchikova, T. A., Kochukhov, O., & Bagnulo, S. 2008, *A&A*, in press (astro-ph/0801.2245)
- Samus, N. N., & Durlевич, O. V. 2004, *VizieR Online Data Catalog*, 2250
- Savanov, I. S. 1995, *Astronomy Letters*, 21, 684
- Shulyak, D., Tsymbal, V., Ryabchikova, T., Stütz, Ch., & Weiss, W. W. 2004, *A&A*, 428, 993
- Sills, A., Pinsonneault, M. H., & Terndrup, D. M. 2000, *ApJ*, 534, 335
- Talon, S., Richard, O., & Michaud, G. 2006, *ApJ*, 645, 634
- Tassoul, J.-L., & Tassoul, M. 1982, *ApJS*, 49, 317

Online Material

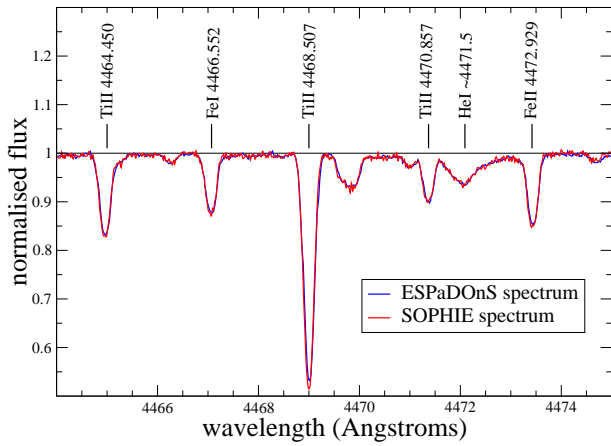


Fig. 13. Comparison between the spectra of HD 73666 obtained with the ESPaDOnS spectropolarimeter (blue line) and the SOPHIE spectrograph (red line) in the region of the He I multiplet at $\sim 4471.5 \text{ \AA}$. No difference is visible between the two spectra, apart the one due to the different spectral resolution of the two instruments.

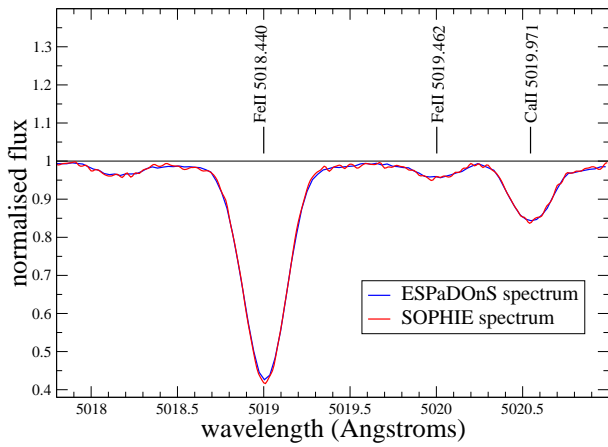


Fig. 14. Same as for Fig. 13, but in the region of the strong Fe II line at 5018.440 \AA .

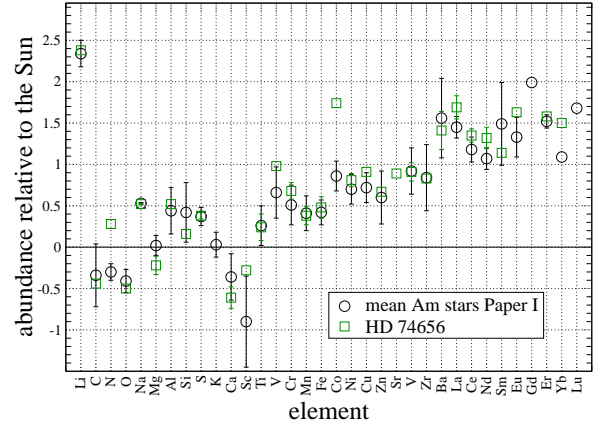


Fig. 15. Comparison between the mean abundance of the Am stars analysed in Paper I and the Am star HD 74656. This plot confirms the Am classification of this star.

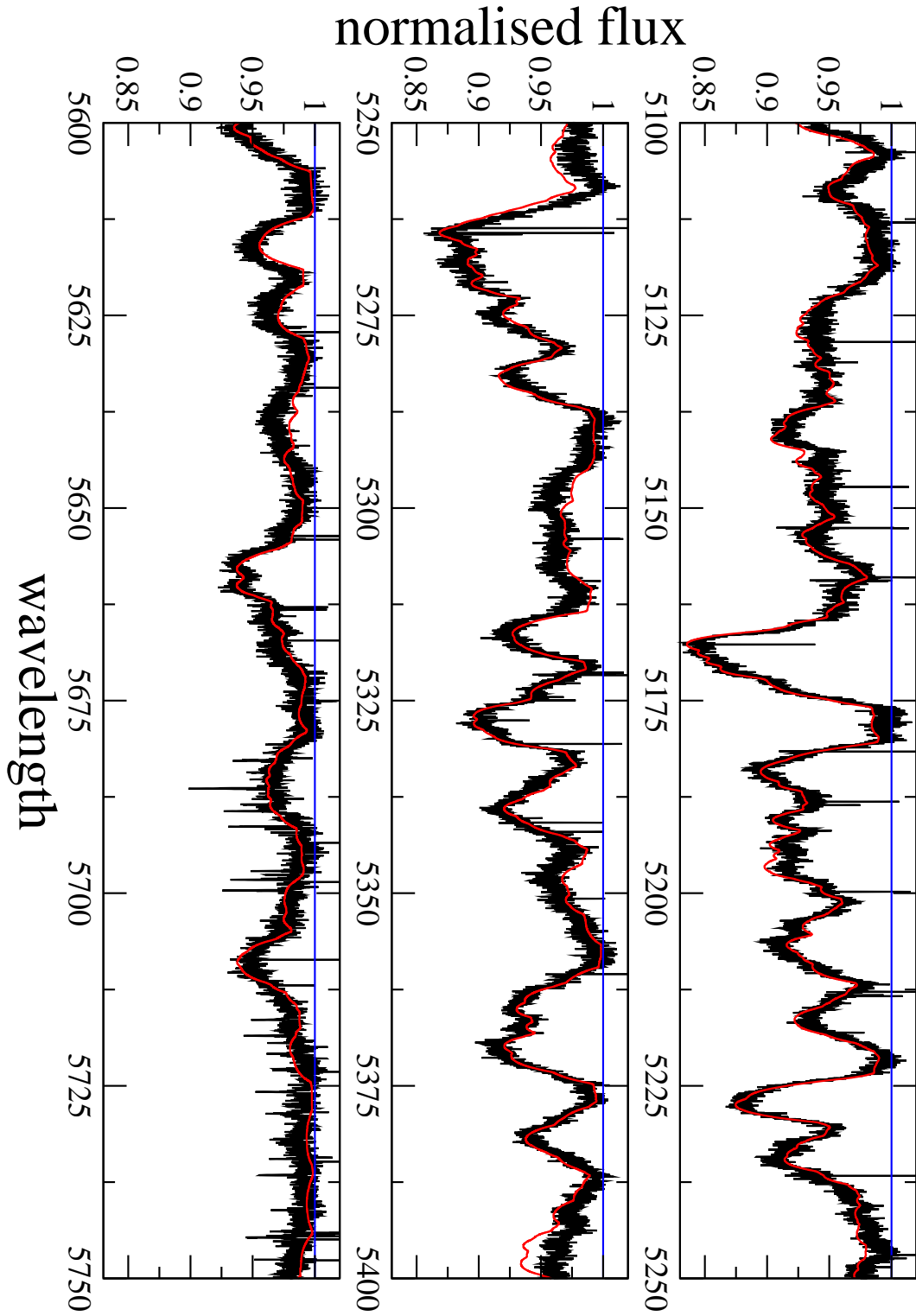


Fig. 16. Portion of the spectrum of HD 72757 ($v \sin i = 179 \text{ km s}^{-1}$) and the synthetic spectrum after the complete abundance analysis in black and red respectively.